

PRESSURE AS A KINETIC PARAMETER IN THE ELUCIDATION OF THE MECHANISMS OF INORGANIC, ORGANOMETALLIC AND BIOINORGANIC REACTIONS IN SOLUTION

Rudi van Eldik

Institute for Inorganic Chemistry - University of Witten/Herdecke - Stockumer Straße 10 - 5810 Witten - Germany

Recebido em 22/7/93

The application of high pressure kinetic techniques in mechanistic studies of chemical reactions in solution, can contribute towards the elucidation of the underlying reaction mechanisms. The fundamental principles involved, the general instrumentation employed, and the construction of reaction volume profiles, are discussed. Typical examples covering various types of reactions in inorganic, organometallic and bioinorganic chemistry, that occur on a range of different time scales, are presented. The advantages of pressure as a kinetic parameter are considered and an evaluation of the gained mechanistic insight is given.

Keywords: high pressure kinetic techniques; mechanistic studies.

INTRODUCTION

The author recently had the privilege to visit a number of Universities in the State of São Paulo and to lecture on the topic of this paper¹. Since this topic is to some extent a new area for Brazilian chemists, the idea originated to compile a concise and generally written review to present a short overview of the principles involved, and to illustrate them with a number of examples selected from inorganic, organometallic and bioinorganic systems. This presentation requires a basic knowledge on inorganic reaction mechanisms as found in a number of general textbooks².

The development of rapid kinetic techniques for the investigation of fast chemical processes in the nanosecond to the second time range at pressures up to 300 MPa (i.e. 3 kbar)³, has opened the possibility to study the effect of pressure on many chemical processes that occur on transition metal complexes. The application of stopped-flow, T-jump, NMR line-broadening, flash-photolysis and pulse-radiolysis, has led to the construction of reaction volume profiles for such processes, which in turn has contributed significantly to the elucidation of the underlying reaction mechanisms. A number of examples dealing with inorganic, organometallic and bioinorganic systems will be treated here. For further information readers are referred to a series of books⁴, conference proceedings⁵ and review papers⁶.

In principle, it has been found that reactions that involve bond formation or bond cleavage, or major changes in electrostriction, exhibit characteristic pressure dependencies. These can along with the data obtained from chemical (concentration, pH, solvent, ionic strength) and physical (temperature) variables be used to resolve the intimate nature of the underlying reaction mechanism. The quantitative description of such pressure dependencies is done in terms of the volume of activation, ΔV^\ddagger , as given in eq. (1), which represents the change in partial molar volume when the reactant species move from the ground to the transition state in terms of the Eyring theory. ΔV^\ddagger will have positive or negative values depending on whether the reaction is decelerated or accelerated

$$(\delta \ln k / \delta P)_T = -\Delta V^\ddagger / RT \quad (1)$$

by pressure, i.e. whether the volume increases or decreases from the ground to the transition state, respectively. Such data

combined with partial molar volume measurements for reactant and product species, or with reaction volume data for an equilibrium process, can be employed to construct a volume profile in which the chemical process is described in terms of volume changes along the reaction coordinate as shown in Figure 1. In this example the solid line represents the expected volume profile for a bond formation process in which the transition state lies between that of the reactant and product states, whereas the dotted lines represent alternative reaction routes in which the transition state has either a higher or lower partial molar volume than both the reactant and product states.

In general, ΔV^\ddagger may be considered as the sum of at least two components: an intrinsic part ($\Delta V^\ddagger_{\text{intr}}$), which represents the change in volume due to changes in bond lengths and angles, and a solvational part ($\Delta V^\ddagger_{\text{solv}}$), which represents the volume changes due to electrostriction and other effects acting on the surrounding solvent molecules during the activation process. It is principally the intrinsic contribution that is the mechanistic indicator in the case of substitution and related reactions. A schematic representation of these components for a typical bond formation or bond cleavage process, during which charge neutralization or creation may occur, is

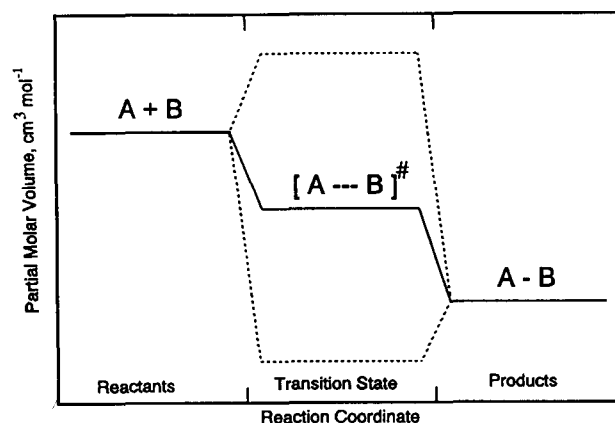


Figure 1. Volume profile for the reaction $A + B \rightleftharpoons [A---B]^\ddagger \rightarrow A-B$.

given in Figure 2. The mechanistic assignment for processes in which no major solvational changes occur are on the basis of the observed ΔV^\ddagger values rather straightforward. In reactions with large changes in electrostriction, $\Delta V_{\text{solv}}^\ddagger$ may be so large that it will counteract and swamp out the $\Delta V_{\text{intr}}^\ddagger$ contribution.

We will now consider a few examples in more detail that cover various types of reactions in inorganic (coordination), organometallic and bioinorganic chemistry, viz. ligand substitution, ligation, electron-transfer, and addition and related processes.

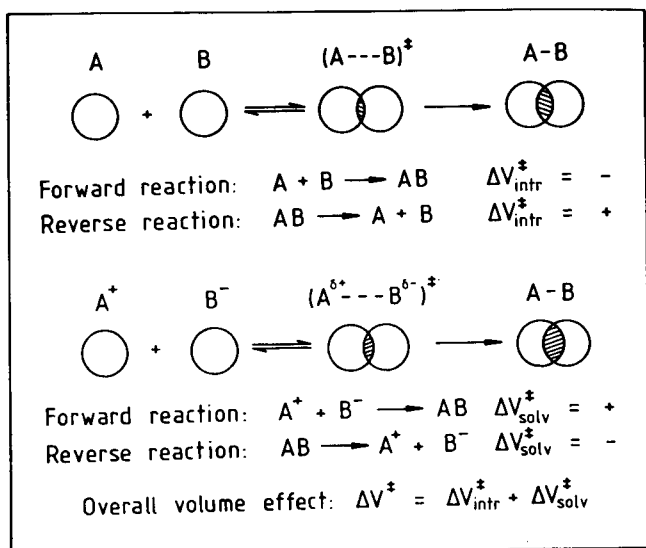


Figure 2. Schematic representation to illustrate the sign of the components of ΔV^\ddagger .

LIGAND SUBSTITUTION REACTIONS

Substitution reactions of transition metal complexes have been the topic of many mechanistic investigations because of the fundamental importance of such reactions in many chemical, biological and catalytic processes. For a general ligand substitution reaction (2), where X is the leaving group and Y the



entering ligand, there are three simple pathways: (i) the dissociative (D) process, with an intermediate of lower coordination number; (ii) the associative (A) process, with an intermediate of higher coordination number; (iii) the interchange (I) process, in which no intermediate of lower or higher coordination number is involved, and the interchange of the two ligands can be more dissociative (I_d) or more associative (I_a) in nature, depending on whether bond breakage or bond formation is more important, respectively (Figure 3)⁷. Such ligand substitution processes should exhibit characteristic ΔV^\ddagger values depending on the degree of bond breaking or bond formation in the transition state. For solvent- and neutral ligand-exchange reactions, i.e. where no net chemical reaction occurs, changes in electrostriction will be negligible and $\Delta V^\ddagger \approx \Delta V_{\text{intr}}^\ddagger$. Thus ΔV^\ddagger should be a direct measure of the intrinsic volume changes that occur, such that a continuous spectrum of transition state configurations can be envisaged, ranging from a very expanded, highly dissociative one (large positive ΔV^\ddagger), to a very compact, highly associative one (large negative ΔV^\ddagger) as shown in Figure 4^{6b}.

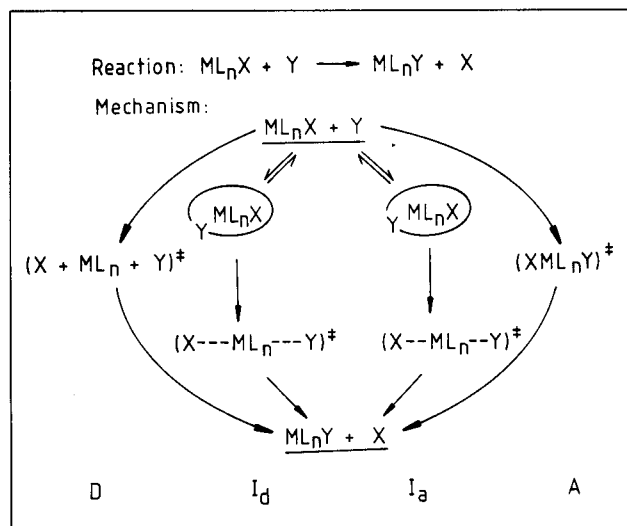


Figure 3. Schematic representation of the possible ligand substitution mechanisms.

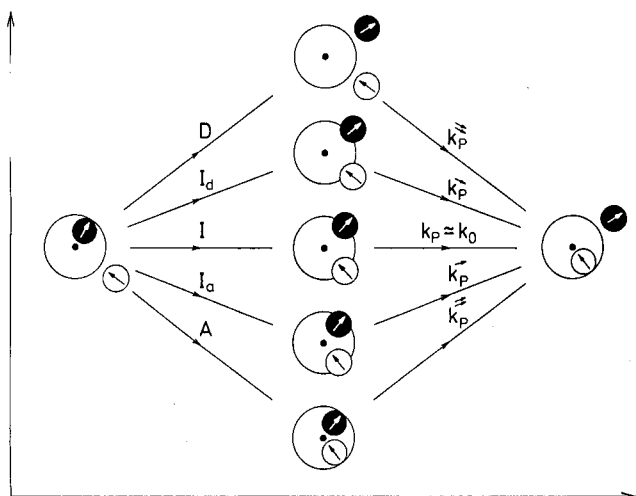


Figure 4. Volume profiles for solvent exchange mechanisms.

Typical experiments on water exchange reactions on octahedral high spin divalent first row transition metal ions employing high pressure NMR techniques, indicated a definite trend along the series of ions (Figure 5)^{6c}. The ΔV^\ddagger data (Table I) indicate that the mechanism progressively changes from I_a

Table I. Volumes of activation ($\text{cm}^3\text{mol}^{-1}$) for solvent S exchange on MS_6^{+2} of the first row transition metal series^{6b}.

M^{2+}	V	Mn	Fe	Co	Ni	Cu
r/pm	79	83	78	74	69	(73)
	t_2g^3	$t_2g^3e_g^2$	$t_2g^4e_g^2$	$t_2g^5e_g^2$	$t_2g^6e_g^2$	$(t_2g^6e_g^3)$
H ₂ O	-4.1	-5.4	+3.8	+6.1	+7.2	
MeOH		-5.0	+0.4	+8.9	+11.4	+8.3
MeCN		-7.0	+3.0	+8.1	+8.5	
DMF		+2.4	+8.5	+9.2	+9.1	
NH ₃					+5.9	

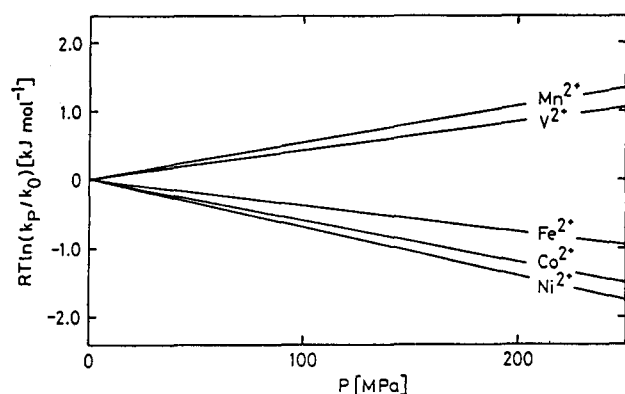


Figure 5. Influence of pressure on the water exchange rate constant for octahedral high spin divalent first row transition metal ions.

for the early to I_d for the later elements, which can be explained by the progressive filling of the d orbitals and the decrease in ionic radii along the series. The small positive ΔV^\ddagger found for DMF exchange on Mn^{2+} , a value that was measured by three independent research groups, indicates that the bulkiness of the coordinated solvent molecules also plays a crucial role in controlling the degree of bond formation/bond breakage in the transition state. In addition, ΔV^\ddagger exhibits a remarkable sensitivity for electronic effects, for instance in the case of induced solvent exchange reactions. Typically, ΔV^\ddagger for water exchange on $Fe(H_2O)_6^{3+}$ has a value of $-5.4 \text{ cm}^3 \text{ mol}^{-1}$, compared to a value of $+7.0 \text{ cm}^3 \text{ mol}^{-1}$ for the 750 times faster (at 25°C) water exchange reaction on $Fe(H_2O)_5OH^{2+}$ ^{6b}. Similarly, ΔV^\ddagger for solvent exchange on $Cr(H_2O)_6^{3+}$, viz. $-9.6 \text{ cm}^3 \text{ mol}^{-1}$, is significantly smaller than for the induced solvent exchange on $Cr(H_2O)_5OH^{2+}$, viz. $+2.7 \text{ cm}^3 \text{ mol}^{-1}$ ^{6b}. Thus the trans-labilization effect of coordinated hydroxide causes a changeover from I_a to I_d or I type of mechanisms, i.e. a more positive ΔV^\ddagger . The rate enhancement observed for acetonitrile exchange in going from $Ru(\eta^6-C_6H_6)(CH_3CN)_3^{2+}$ to $Ru(\eta^5-C_5H_5)(CH_3CN)_3^{2+}$ is also accompanied by a significant increase in ΔV^\ddagger and a changeover in mechanism from I to D , respectively⁸.

Non-symmetrical ligand substitution reactions, for which the overall reaction volume $\Delta V^\ddagger \neq 0$, exhibit pressure dependencies that correlate closely with those found for solvent exchange processes in the case of complex formation reactions^{6c}. The corresponding volume profiles illustrate the looseness or compactness of the transition state during the ligand substitution process. Such volume profiles can for instance be used to investigate a possible changeover in mechanism caused by increasing steric hindrance in substitution reactions of square planar d^8 metal complexes, that are usually accepted to follow an associative mechanism. For instance the introduction of methyl and ethyl substituents on the diethylenetriamine ligand of $Pd(II)$ complexes causes a decrease of up to 6 orders of magnitude in the substitution rate constant, but does not affect the nature of the mechanism since both ΔS^\ddagger and ΔV^\ddagger values remain strongly negative^{6c}. Two representative volume profiles are given in Figure 6, from which it follows that the transition state has a significantly lower partial molar volume than either the reactant or product states, demonstrating the associative character of the substitution process^{4b}.

Ligand substitution reactions of a number of organometallic complexes and clusters have also been investigated using high pressure kinetic techniques. For instance, the substitution of coordinated CO by $P(OMe)_3$ on $Cr(CO)_4phen$, phen = 1,10 phenanthroline, is characterized by a ΔV^\ddagger of $+13.8 \pm 0.5$

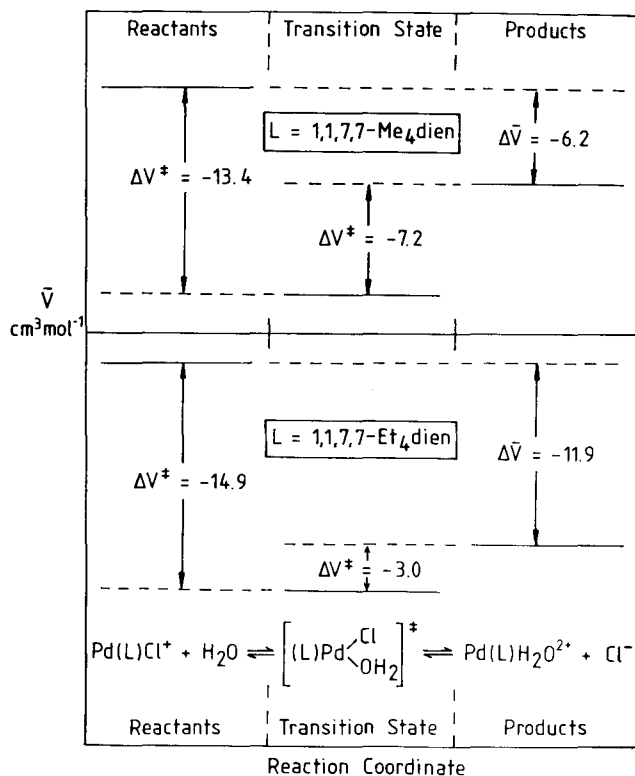


Figure 6. Volume profiles for the reaction $Pd(L)Cl + H_2O \rightleftharpoons Pd(L)H_2O^{2+} + Cl^-$.

$\text{cm}^3 \text{ mol}^{-1}$, whereas the reverse reaction exhibits a ΔV^\ddagger of $+19.2 \pm 0.5 \text{ cm}^3 \text{ mol}^{-1}$ ⁹. The volume profile for this process (Figure 7) clearly demonstrates the significantly higher partial molar volume of the transition state and the operation of a dissociative (D) mechanism. The overall reaction volume is slightly negative and indicates an overall volume decrease during the substitution process. A number of studies on photo-induced substitution reactions of metal carbonyl complexes that involve the displacement of coordinated solvent molecules, or the subsequent displacement of coordinated CO when the entering ligand is a bidentate species^{6c}, clearly demonstrate the sensitivity of ΔV^\ddagger , and therefore the underlying mechanism, on the

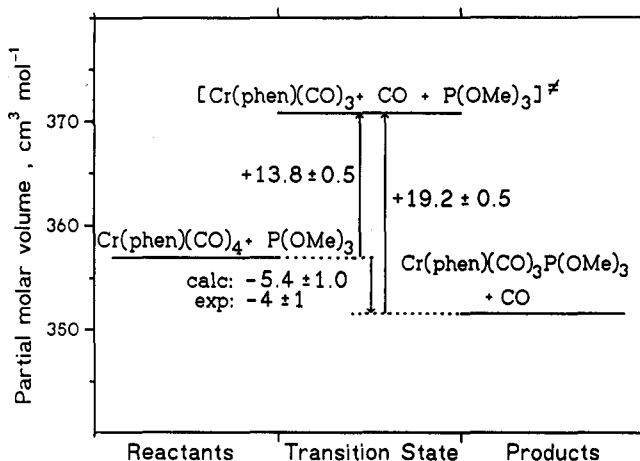
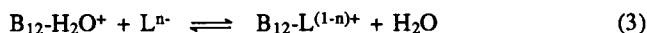


Figure 7. Volume profile for the reaction $Cr(phen)(CO)_4 + P(OMe)_3 \rightleftharpoons Cr(phen)(CO)_3P(OMe)_3 + CO$.

size of the central metal and the steric hindrance on the coordinating nucleophiles. In a similar way, ligand substitution reactions that occur in the electronically excited state of organometallic complexes also exhibit very characteristic pressure dependencies¹⁰. In general ligand field excitation is characterized by dissociative substitution reactions and positive ΔV^\ddagger values, whereas metal to ligand charge transfer excitation is characterized by associative substitution reactions and negative ΔV^\ddagger values.

Ligand substitution reactions of cobalamins (Vitamin B₁₂) has also attracted attention of high pressure kineticists. In these systems the usually kinetic inert Co(III) center is considerably labilized by the corrin ring, and there has been some disagreement in the literature concerning the mechanism of these substitution reactions^{6c}. The observed ΔV^\ddagger for the forward and reverse reactions in (3) did not allow an unequivocal assignment of the mechanism in terms of I_d or D. For the reaction with pyridine (py) the observed rate constant



reached a limiting value at high pyridine concentrations, which has now been interpreted in terms of a precursor formation step followed by a rate-determining ligand exchange process, i.e. an I_d mechanism, for which the corresponding volume profile is presented in Figure 8^{5c}. The significantly higher partial molar volume of the transition state compared to the reactant and product states, demonstrates the dissociative character of the interchange process.

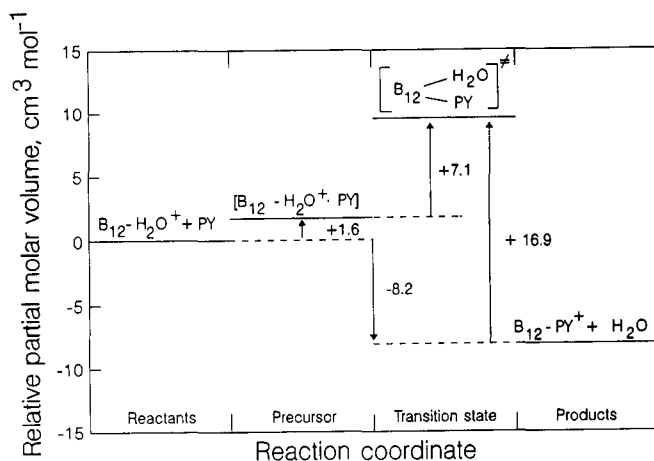


Figure 8. Volume profile for the reaction $B_{12}\text{-H}_2\text{O}^+ + \text{py} \rightleftharpoons B_{12}\text{-py}^+ + \text{H}_2\text{O}$.

The development of high-pressure pulse-radiolysis techniques^{6c} has enabled the possibility to study the formation of metal-carbon bonds and the associated volume changes. Such processes are closely related to ligand substitution reactions since the aliphatic free radical (produced via pulse-radiolysis) must substitute a solvent molecule (usually water) on the metal center to produce the metal-carbon σ bond. A volume profile for the reaction of $\text{Co}^{\text{II}}(\text{nta})(\text{H}_2\text{O})_2$ (nta = nitrilotriacetate) with $\bullet\text{CH}_3$ to produce $\text{Co}^{\text{III}}(\text{nta})(\text{H}_2\text{O})\text{CH}_3$ ^{5c} clearly indicated that the process is controlled by solvent exchange on the $\text{Co}^{\text{II}}(\text{nta})(\text{H}_2\text{O})_2$ species that follows an I_d mechanism. Subsequently, the effect of pressure on the formation of a series of organo-chromium(III) species were studied in an effort to obtain mechanistic information on solvent exchange and complex formation reactions of $\text{Cr}(\text{H}_2\text{O})_6^{2+}$. This reaction was

studied for 10 different aliphatic radicals $\bullet\text{R}$, which all exhibited very similar complex formation rate constants and small positive ΔV^\ddagger values with an average of $+4.3 \pm 1.0 \text{ cm}^3\text{mol}^{-1}$, independent of the nature of R¹¹. These values suggested that Cr-C bond formation is controlled by solvent exchange on $\text{Cr}(\text{H}_2\text{O})_6^{2+}$, which follows an I_d mechanism, and a typical volume profile is reported in Figure 9. Thus breakage of the Cr^{II}-H₂O bond accounts for the volume increase in going to the transition state, which is followed by a significant volume collapse due to Cr-C bond formation and the contraction due to $\text{Cr}^{\text{II}}\text{-R} \rightarrow \text{Cr}^{\text{III}}\text{-R}$.

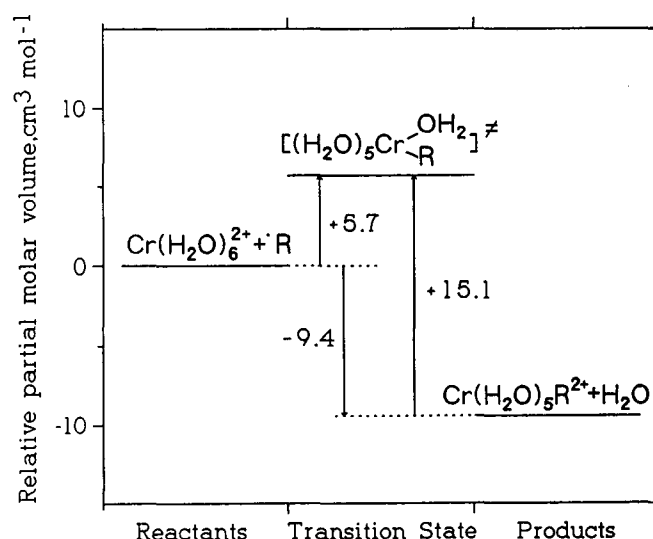
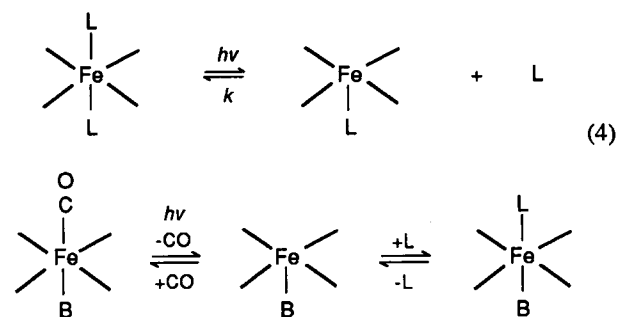


Figure 9. Volume profile for the reaction $\text{Cr}(\text{H}_2\text{O})_6^{2+} + \bullet\text{C}(\text{H}_3)_2\text{OH} \rightleftharpoons \text{Cr}(\text{H}_2\text{O})_5\text{C}(\text{H}_3)_2\text{OH}^{2+} + \text{H}_2\text{O}$.

LIGATION REACTIONS

The mechanistic understanding of the binding of small molecules such as O₂, CO and NO to ferrous hemes and hemoproteins has received significant attention from kineticists. Such processes control the overall transport of such molecules in biological systems. The flash photolysis techniques outlined in (4) have been used to study ligand binding to two model heme systems, viz. protoheme dimethyl ester (PHDME) and monochelated protoheme [MCPH]^{12a}, and the effect of pressure on such processes is reported in Table II.



The data show a clear correlation between ΔV^\ddagger and k_{on} , viz. for the slower reactions recombination of the separated pair is rate-limiting (negative ΔV^\ddagger value), whereas for the faster reactions the process becomes diffusion controlled in toluene and slows down with increasing pressure due to the increase

Table II. ΔV^\ddagger data for the bimolecular addition of various neutral ligands to five-coordinate ferrous model heme complexes in toluene as solvent^{12a}.

Heme complex	L	$k_{on}(25\text{ }^\circ\text{C})$ $\text{M}^{-1}\text{s}^{-1}$	ΔV^\ddagger $\text{cm}^3\text{mol}^{-1}$
MCPH	CO	1.1×10^7	-19.3 ± 0.4
MCPH	O ₂	1.1×10^7	-11.3 ± 1.0
(MeNC) PHDME	MeNC	3.9×10^8	$+11.6 \pm 0.8$
(t-BuNC) PHDME	t-BuNC	2.5×10^8	$+9.9 \pm 1.0$
(1-MeIm) PHDME	1-MeIm	1.5×10^8	$+10.9 \pm 3.1$

in viscosity of toluene. When the reaction of CO with MCPH is studied as a function of pressure in a highly viscous medium, viz. 90/10 (v/v) mineral oil/toluene, the observed recombination rate constant shows a changeover in rate-determining step with increasing pressure^{12b}. In the low pressure range bond formation is rate-determining and ΔV^\ddagger is negative, whereas in the high pressure range diffusion becomes rate-determining and ΔV^\ddagger is positive.

Similar techniques were applied to study the pressure dependence of the bimolecular association rate constant for the reaction of sperm whale myoglobin with O₂ and CO. Surprisingly, the slower binding of CO ($5 \times 10^5 \text{ M}^{-1}\text{s}^{-1}$ at 25 °C) exhibits a ΔV^\ddagger of $-10 \text{ cm}^3\text{mol}^{-1}$, but the faster binding of O₂ ($1 \times 10^7 \text{ M}^{-1}\text{s}^{-1}$ at 25 °C) exhibits a ΔV^\ddagger of $+8 \text{ cm}^3\text{mol}^{-1}$ ^{12a}. This apparent discrepancy motivated us to perform a detailed volume profile analysis for both reactions^{12c,d}. T-jump techniques were used to study the binding of O₂ and CO to deoxymyoglobin (Mb), whereas the reverse reactions, i.e. the release of O₂ and CO, were studied using a stopped-flow technique in which O₂ and CO were rapidly removed from the equilibrium mixture in a chemical way. In addition, the pressure dependence of the overall equilibrium constant was studied using UV-VIS techniques. From the ΔV^\ddagger data for the "on" and "off" reactions the overall reaction volume could be calculated, viz. $\Delta \bar{V} = \Delta V^\ddagger_{on} - \Delta V^\ddagger_{off}$, which turned out to be in good agreement with the directly determined value. These data could now be employed to construct a volume profile for the reaction of myoglobin with O₂ and CO, which have been combined in Figure 10. The volume profile for the binding of O₂ is characterized by the unexpected volume increase in going from the reactant to the transition state, as observed in the flash photolysis experiments, followed by a significant vol-

ume collapse in going to the product state. The observed volume increase has been ascribed to rate-determining movement of O₂ through the protein to the heme pocket, which may involve desolvation, some opening up of the protein as well as significant hydrogen bond formation with the distal histidine^{12c}. This is followed by rapid bond formation with the Fe(II) center, during which the metal center changes from high spin to low spin, the Fe(II) moves into the porphyrin plane, and some conformational changes on the protein may occur. These effects all add up to a large volume collapse of $-23 \text{ cm}^3\text{mol}^{-1}$ observed from the transition state to the product state. The overall reaction volume of $-18 \text{ cm}^3\text{mol}^{-1}$ demonstrates the large volume collapse caused by the bonding of O₂. The volume profile for the binding of CO shows the expected volume decrease for rate-determining bond formation on going from the reactant to the transition state. Surprisingly, the reverse bond cleavage process is accompanied by a volume decrease, which may be related to the significantly different bonding mode of CO compared to O₂. It is known that the porphyrin iron binds O₂ under an angle of 115 ° and exhibits hydrogen bonding to histidine E7, which results in a sterically favoured orientation of O₂ in the porphyrin pocket. In contrast, CO does not show any hydrogen bonding, and its favoured linear bonding geometry is not possible due to histidine E7. This causes the heme pocket to widen significantly as compared to deoxymyoglobin due to steric tension. It follows that Fe-CO bond breakage will be accompanied by a decrease in steric tension and an associated volume collapse due to reorganization of the protein pocket as CO leaves the iron coordination site. This significantly different bonding mode of CO must also account for the much higher partial molar volume of MbCO and the much smaller absolute reaction volume observed for the binding of CO, viz. $-6 \text{ cm}^3\text{mol}^{-1}$, than for the binding of O₂.

ELECTRON-TRANSFER REACTIONS

Electron-transfer reactions of transition metal complexes are accompanied by a change in the oxidation state of the metal atom and the overall charge on the complex ion. This causes both intrinsic and solvational volume changes, such that it is reasonable to expect that electron-transfer reactions should exhibit characteristic ΔV^\ddagger values. In the case of symmetrical intermolecular reactions, the ΔV^\ddagger data can also be accounted for theoretically on the basis of the Marcus-Hush-Stranks treatment^{6c}. A typical example is the self-exchange reactions of $\text{Fe}(\text{H}_2\text{O})_6^{2+/3+}$ and $\text{Fe}(\text{H}_2\text{O})_5\text{OH}^{2+}/\text{Fe}(\text{H}_2\text{O})_6^{2+}$ for which ΔV^\ddagger has the values -11 and $+1 \text{ cm}^3\text{mol}^{-1}$, respectively¹³. These values can be accounted for essentially quantitatively on the basis of an adiabatic intermolecular mechanism for the former and a hydroxo-bridged intramolecular mechanism that involves the release of a solvent molecule for the latter process.

In the case of non-symmetrical intermolecular reactions between complexes of the type $\text{Co}^{\text{III}}(\text{NH}_3)_5\text{X}^{(3-n)+}$ and $\text{Fe}(\text{CN})_6^{4-}$, ΔV^\ddagger usually has large positive values, which can be accounted for in terms of a large decrease in electrostriction due to charge neutralization, $\text{Co}^{\text{III}} \rightarrow \text{Co}^{\text{II}}$ and $\text{Fe}(\text{CN})_6^{4-} \rightarrow \text{Fe}(\text{CN})_6^{3-}$ ^{5c, 6c}. Similarly, the oxidation of L-ascorbic acid and the ascorbate ion by $\text{Fe}(\text{CN})_6^{3-}$ exhibits ΔV^\ddagger values of ca. $-16 \text{ cm}^3\text{mol}^{-1}$, which can again be accounted for in terms of the increase in electrostriction when $\text{Fe}(\text{CN})_6^{3-}$ is reduced to $\text{Fe}(\text{CN})_6^{4-}$ ^{14a}. Similar studies for the oxidation of L-ascorbic acid by $\text{Fe}(\text{H}_2\text{O})_6^{3+}$ and $\text{Fe}(\text{H}_2\text{O})_5\text{OH}^{2+}$ indicate ΔV^\ddagger values of $+14$ and $+5 \text{ cm}^3\text{mol}^{-1}$, respectively^{14b}. For the less labile $\text{Fe}(\text{H}_2\text{O})_6^{3+}$ species it was suggested that the redox process follows an intermolecular route, such that the significant volume increase will be related to the reduction of $\text{Fe}(\text{H}_2\text{O})_6^{3+}$ to $\text{Fe}(\text{H}_2\text{O})_6^{2+}$. In the case of the more labile $\text{Fe}(\text{H}_2\text{O})_5\text{OH}^{2+}$ species, it was suggested that complex formation is rate-deter-

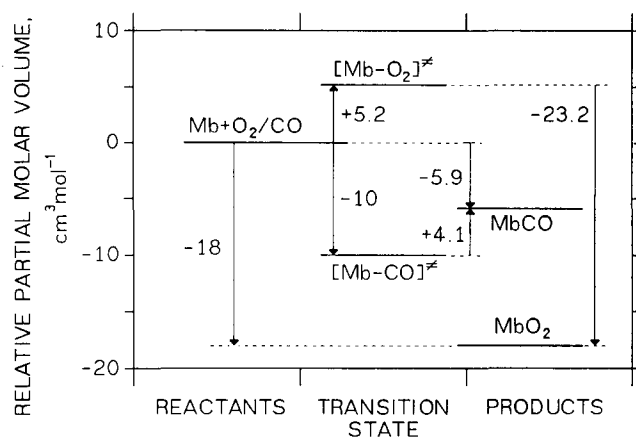


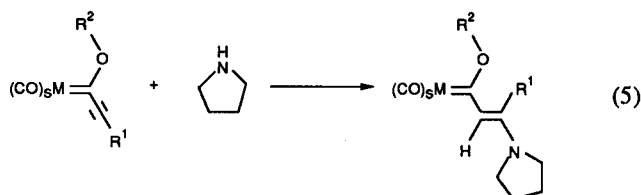
Figure 10. Comparison of the volume profiles for the reactions $\text{Mb} + \text{O}_2 \rightleftharpoons \text{MbO}_2$ and $\text{Mb} + \text{CO} \rightleftharpoons \text{MbCO}$.

mining, followed by a rapid intramolecular electron-transfer reaction, such that ΔV^\ddagger correlates with that found for solvent exchange on $\text{Fe}(\text{H}_2\text{O})_5\text{OH}^{2+}$. Recent work has shown that long-distance electron-transfer reactions between Ru(II) complexes and ferri cytochrome c exhibit ΔV^\ddagger values between -16 and -18 $\text{cm}^3\text{mol}^{-1}$ for both intermolecular and intramolecular processes^{5c, 14c}. These values are once again assigned to the significant increase in electrostriction when Ru^{II} is oxidized to Ru^{III}^{14c}.

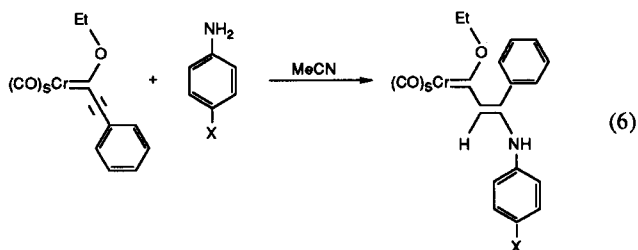
ADDITION AND RELATED PROCESSES

Up to now we have seen that bond formation processes are characterized by negative ΔV^\ddagger values, and it is therefore not surprising that oxidative addition reactions are characterized by significantly negative ΔV^\ddagger values, partly due to bond formation and partly due to a decrease in the size of the metal center during the oxidation process^{6b}. Typical ΔV^\ddagger values can be as large as -30 to -40 $\text{cm}^3\text{mol}^{-1}$, and exhibit a strong solvent dependence due to the significant electrostriction contribution.

It was recently shown that [2+2] cyclo-addition reactions on the coordinated ligand of pentacarbonyl carbene complexes of Cr and W, as well as insertion reactions into the metal-carbene bond of pentacarbonyl(carbene)chromium and -tungsten complexes, all exhibit ΔV^\ddagger values between -15 and -25 $\text{cm}^3\text{mol}^{-1}$ ^{15a,b}. It follows that such processes are in general accelerated by pressure, which could have some synthetic application^{4c}. Addition reactions of α,β -unsaturated Fischer carbene complexes shown in (5) exhibit ΔV^\ddagger values around -16 $\text{cm}^3\text{mol}^{-1}$ in acetonitrile, which become more negative in



going to less polar solvents^{15c}. These data exhibit a good correlation with the solvent parameter q_p (i.e. the pressure derivative of q) as shown in Figure 11, from which it follows that the intercept, $\Delta V^\ddagger_{\text{intr}}$, has a value of ca. -14 $\text{cm}^3\text{mol}^{-1}$. A similar study for the addition of a series of *p*-substituted anilines to a Fischer carbene complex as shown in (6), resulted in the data summarized in Table III^{15d}.



The observed second order rate constant shows a good correlation with the increase in basicity of the amine, which is accompanied by a significant decrease in ΔH^\ddagger and an increase in ΔV^\ddagger to more positive values. These trends demonstrate that the slow reactions (high ΔH^\ddagger) occur via a late transition state (strongly negative ΔV^\ddagger), whereas the fast reactions (low ΔH^\ddagger) occur via an early transition state (more positive ΔV^\ddagger). This demonstrates the usefulness of combined ΔH^\ddagger and ΔV^\ddagger data to obtain information on the location of the transition state in terms of "early" or "late", as illustrated schematically in Figure 12.

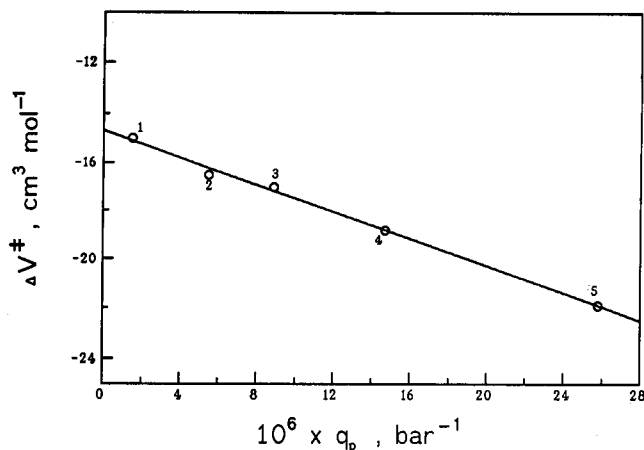


Figure 11. Plot of ΔV^\ddagger versus qp for reaction (5) with $M = \text{W}$, $R^1 = \text{Ph}$ and $R^2 = \text{Et}$. Solvents: acetonitrile (1), 1,2-dichlorobenzene (2), chlorobenzene (3), benzene (4), *n*-heptane (5).

Table III. Summary of rate and activation parameters for the addition of *p*-substituted anilines to Fischer carbenes^{15d}.

<i>p</i> -substituent	$\text{p}K_a$ (H_2O)	$k \times 10^2$ $\text{M}^{-1}\text{s}^{-1}$	ΔH^\ddagger kJ mol^{-1}	ΔS^\ddagger $\text{J K}^{-1}\text{mol}^{-1}$	ΔV^\ddagger $\text{cm}^3\text{mol}^{-1}$
CN	1.74	0.69	29 ± 3	-190 ± 9	-27.9 ± 0.6
CH_3CO	2.75	2.8	29 ± 2	-179 ± 8	-26.6 ± 0.5
Cl	3.99	21	26 ± 2	-169 ± 6	-24.5 ± 0.4
H	4.63	73	24 ± 1	-167 ± 5	-22.2 ± 0.8
F	4.65	65	23 ± 1	-172 ± 4	-24.6 ± 0.9
CH_3	5.08	167	24 ± 2	-159 ± 8	-21.1 ± 1.0
CH_3O	5.36	497	18 ± 2	-170 ± 6	-21.1 ± 1.0

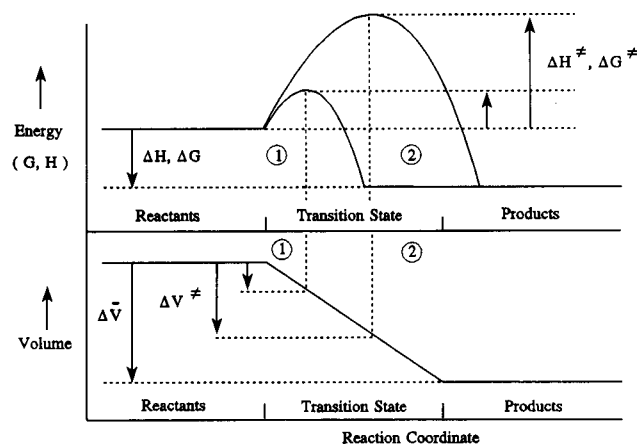


Figure 12. Schematic presentation of the concept of an "early" and "late" transition state in terms of enthalpy and volume effects along the reaction coordinate.

CONCLUSIONS

The analysis of a chemical process in terms of volume changes along the reaction coordinate can help us to visualize the nature and structure of the transition state in terms of intrinsic and solvational changes in partial molar volume. With the data presently available, intrinsic volume changes in in-

organic, organometallic and bioinorganic systems are fairly well understood and can be interpreted with confidence. This is, however, not the case for solvational volume changes and much more work is required to resolve the origin of all the observed effects. There are many cases in which it is experimentally impossible to construct a volume profile, for instance due to the occurrence of subsequent reactions or the irreversibility of the process as found in many electron-transfer and photo-induced reactions. Nevertheless, the volumes of activation for such processes can still be employed very successfully to gain information on the nature of the transition state.

It is important to realize that the presented interpretations of ΔV^\ddagger data are all based on a simplified version of the transition state theory, which has its limitations and restrictions, and various modifications are being discussed. Notwithstanding this complication that also concerns the interpretation of the temperature dependence of a chemical reaction, it is clear from the given examples that the additional physical parameter pressure has added a decisive dimension to mechanistic studies of inorganic, organometallic and bioinorganic reactions in solution. The fact that the rate-determining step of a particular process exhibits a characteristic pressure dependence, creates the possibility to tune the reactivity of particular systems via the application of moderate pressures. This can for instance lead to the selective synthesis of particular reaction products in cases where product distribution proves to be pressure dependent, or to the optimization of the design of industrial chemical reactions.

It is the authors personal opinion that when dealing with mechanistic studies in general, one should investigate as many chemical and physical variables as possible in order to obtain as much indirect information as possible on the nature of the underlying reaction mechanism. Only then can the suggested mechanism come close to the "real" mechanism, which is a goal set by many kineticists but not always accomplished. If we can contribute in this way to a better understanding of the mechanism of chemical reactions in solution, then we have fulfilled our educational commitments and have added a drop to the bucket of existing knowledge.

ACKNOWLEDGEMENTS

The author gratefully acknowledges financial support from the Deutsche Forschungsgemeinschaft, Fonds der Chemischen Industrie, Volkswagen-Stiftung, NATO Scientific Affairs Division and the German-Israeli Foundation. The very stimulating collaboration with numerous graduate students, post docs, visiting scientists and various groups all over the world is highly appreciated.

REFERENCES AND NOTES

1. The author gratefully acknowledges financial support from FAPESP and DAAD that enabled this visit. The initiative and excellent hosting by Professor Douglas Franco, Universidade de São Paulo, São Carlos, is highly appreciated.
2. a) Wilkins, R.G.; *Kinetics and Mechanism of Reactions of Transition Metal Complexes*, VCH, Weinheim, 1991;

- b) Atwood, J.L.; *Inorganic and Organometallic Reaction Mechanisms*, Brooks/Cole Publishing Co, Monterey, USA, 1985; c) Jordan, R.B.; *Reaction Mechanisms of Inorganic and Organometallic Systems*, Oxford University Press, New York, 1991.
3. Kotowski, M. and van Eldik, R.; *Coord. Chem. Rev.*, (1989), **93**, 19.
4. a) van Eldik, R.; (Ed.), *Inorganic High Pressure Chemistry. Kinetics and Mechanisms*, Elsevier, Amsterdam, 1986; b) W.J. le Noble (Ed.), *Organic High Pressure Chemistry*, Elsevier, Amsterdam, 1988; c) Jurczak, J. and Baranowski, B.; (Eds.), *High Pressure Chemical Synthesis*, Elsevier, Amsterdam 1989.
5. a) Kelm, H.; (Ed.), *High Pressure Chemistry*, Reidel, Dordrecht, 1978; b) van Eldik, R. and Jonas, J.; (Eds.), *High Pressure Chemistry and Biochemistry*, Reidel, Dordrecht, 1987; c) Winter, R. and Jonas, J.; (Eds.), *High Pressure Chemistry, Biochemistry and Material Science*, in press.
6. a) van Eldik, R. Asano, T. and le Noble, W.J.; *Chem. Rev.*, (1989), **89**, 541; b) Akitt, J.W. and Merbach, A.E.; in *NMR Basic Principles and Progress*; (1990), **24**, 189; c) van Eldik, R. and Merbach, A.E.; *Comments Inorg. Chem.*, (1992), **12**, 341.
7. Langford, C.H. and Gray, H.B.; *Ligand Substitution Processes*, W.A. Benjamin, New York, 1965.
8. Luginbühl, W.; Zbinden, P.; Pittet, P.A.; Armbruster, T.; Bürgi, H.-B.; Merbach, A.E. and Ludi, A.; *Inorg. Chem.*, (1991), **30**, 2350.
9. Schneider, K.J. and van Eldik, R.; *Organometallics*, (1990), **9**, 1235.
10. a) Wieland, S. and van Eldik, R.; *Coord. Chem. Rev.*, (1990), **97**, 155; b) Wieland, S. and van Eldik, R.; *J. Phys. Chem.*, (1990), **94**, 5865; c) Wieland, S.; Bal Reddy, K. and van Eldik, R.; *Organometallics*, (1990), **9**, 1802.
11. van Eldik, R.; Gaede, W.; Cohen, H. and Meyerstein, D.; *Inorg. Chem.*, (1992), **31**, 3695.
12. a) Taube, D.J.; Projahn, H.-D.; van Eldik, R.; Magde, D. and Traylor, T.G.; *J. Am. Chem. Soc.*, (1990), **112**, 6880; b) Traylor, T.G.; Luo, J.; Simon, J. and Ford, P.C.; *J. Am. Chem. Soc.*, (1992), **114**, 4340; c) Projahn, H.-D.; Dreher, C. and van Eldik, R.; *J. Am. Chem. Soc.*, (1990), **112**, 17; d) Projahn, H.-D. and van Eldik, R.; *Inorg. Chem.*, (1992), **30**, 3288.
13. Jolley, W.H.; Stranks, D.R. and Swaddle, T.W.; *Inorg. Chem.*, (1990), **29**, 1948.
14. a) Bäsch, B.; Martinez, P.; Zuluaga, J.; Uribe, D. and van Eldik, R.; *Z. Phys. Chem.*, (1991), **170**, 59; b) Bäsch, B.; Martinez, P.; Uribe, D.; Zuluaga, J. and van Eldik, R.; *Inorg. Chem.*, (1991), **30**, 4555; c) Wishart, J.F.; van Eldik, R.; Sun, J.; Su, C. and Isied, S.S.; *Inorg. Chem.*, (1992), **31**, 3986.
15. a) Pipoh, R.; van Eldik, R.; Wang, S.L.B. and Wulff, W.D.; *Organometallics*, (1992), **11**, 490; b) Schneider, K.J.; Neubrand, A.; van Eldik, R. and Fischer, H.; *Organometallics*, (1992), **11**, 267; c) Pipoh, R.; van Eldik, R. and Henkel, G.; *Organometallics*, in press; d) Pipoh, R. and van Eldik, R.; *Organometallics*, in press.